UCLA
UCLA Previously Published Works

Title

Plasticity of GABAA receptor-mediated neurotransmission in the nucleus accumbens of alcohol-dependent rats

Permalink

https://escholarship.org/uc/item/9n7997s8

Journal

Journal of Neurophysiology, 112(1)

ISSN

0022-3077

Authors

Liang, Jing
Lindemeyer, A Kerstin
Suryanarayanan, Asha
et al.

Publication Date

2014-07-01

DOI

10.1152/jn.00565.2013

Peer reviewed

eScholarship.org Powered by the California Digital Library
University of California

Plasticity of $GABA_A$ receptor-mediated neurotransmission in the nucleus accumbens of alcohol-dependent rats

Jing Liang, A. Kerstin Lindemeyer, Asha Suryanarayanan, Edward M. Meyer, Vincent N. Marty, S. Omar Ahmad, Xuesi Max Shao, Richard W. Olsen and Igor Spigelman

J Neurophysiol 112:39-50, 2014. First published 2 April 2014; doi:10.1152/jn.00565.2013

You might find this additional info useful...

This article cites 81 articles, 38 of which can be accessed free at:
/content/112/1/39.full.html#ref-list-1

This article has been cited by 1 other HighWire hosted articles

Selective modulation of GABAergic tonic current by dopamine in the nucleus accumbens of alcohol-dependent rats
Jing Liang, Vincent N. Marty, Yatendra Mulpuri, Richard W. Olsen and Igor Spigelman
J Neurophysiol, July 1, 2014; 112 (1): 51-60.
[Abstract] [Full Text] [PDF]

Updated information and services including high resolution figures, can be found at:
/content/112/1/39.full.html

Additional material and information about ***Journal of Neurophysiology*** can be found at:
http://www.the-aps.org/publications/jn

This information is current as of July 7, 2014.

Journal of Neurophysiology publishes original articles on the function of the nervous system. It is published 12 times a year (monthly) by the American Physiological Society, 9650 Rockville Pike, Bethesda MD 20814-3991. Copyright © 2014 by the American Physiological Society. ISSN: 0022-3077, ESSN: 1522-1598. Visit our website at http://www.the-aps.org/.

Downloaded from on July 7, 2014

J Neurophysiol 112: 39–50, 2014.
First published April 2, 2014; doi:10.1152/jn.00565.2013.

Plasticity of $GABA_A$ receptor-mediated neurotransmission in the nucleus accumbens of alcohol-dependent rats

Jing Liang,[1,2] A. Kerstin Lindemeyer,[2] Asha Suryanarayanan,[1] Edward M. Meyer,[1] Vincent N. Marty,[1] S. Omar Ahmad,[3] Xuesi Max Shao,[4] Richard W. Olsen,[2] and Igor Spigelman[1]

[1]*Division of Oral Biology and Medicine, School of Dentistry, University of California, Los Angeles, California;* [2]*Department of Molecular and Medical Pharmacology, David Geffen School of Medicine, University of California, Los Angeles, California;* [3]*Doisy College of Health Sciences, Saint Louis University, St. Louis, Missouri; and* [4]*Department of Neurobiology, David Geffen School of Medicine, University of California, Los Angeles, California*

Submitted 8 August 2013; accepted in final form 2 April 2014

Liang J, Lindemeyer AK, Suryanarayanan A, Meyer EM, Marty VN, Ahmad SO, Shao XM, Olsen RW, Spigelman I. Plasticity of $GABA_A$ receptor-mediated neurotransmission in the nucleus accumbens of alcohol-dependent rats. *J Neurophysiol* 112: 39–50, 2014. First published April 2, 2014; doi:10.1152/jn.00565.2013.—Chronic alcohol exposure-induced changes in reinforcement mechanisms and motivational state are thought to contribute to the development of cravings and relapse during protracted withdrawal. The nucleus accumbens (NAcc) is a key structure of the mesolimbic dopaminergic reward system and plays an important role in mediating alcohol-seeking behaviors. Here we describe the long-lasting alterations of γ-aminobutyric acid type A receptors ($GABA_A$Rs) of medium spiny neurons (MSNs) in the NAcc after chronic intermittent ethanol (CIE) treatment, a rat model of alcohol dependence. CIE treatment and withdrawal (>40 days) produced decreases in the ethanol and Ro15-4513 potentiation of extrasynaptic $GABA_A$Rs, which mediate the picrotoxin-sensitive tonic current (I_{tonic}), while potentiation of synaptic receptors, which give rise to miniature inhibitory postsynaptic currents (mIPSCs), was increased. Diazepam sensitivity of both I_{tonic} and mIPSCs was decreased by CIE treatment. The average magnitude of I_{tonic} was unchanged, but mIPSC amplitude and frequency decreased and mIPSC rise time increased after CIE treatment. Rise-time histograms revealed decreased frequency of fast-rising mIPSCs after CIE treatment, consistent with possible decreases in somatic GABAergic synapses in MSNs from CIE rats. However, unbiased stereological analysis of NeuN-stained NAcc neurons did not detect any decreases in NAcc volume, neuronal numbers, or neuronal cell body volume. Western blot analysis of surface subunit levels revealed selective decreases in α1 and δ and increases in α4, α5, and γ2 $GABA_A$R subunits after CIE treatment and withdrawal. Similar, but reversible, alterations occurred after a single ethanol dose (5 g/kg). These data reveal CIE-induced long-lasting neuroadaptations in the NAcc GABAergic neurotransmission.

ventral striatum; ethanol; withdrawal; neuroadaptation; tonic current

ALCOHOL, one of the oldest drugs, is lawfully consumed in our society for its taste, caloric value, and psychoactive properties. However, excessive alcohol drinking can lead to alcohol dependence and loss of control over alcohol consumption, with serious detrimental health consequences (Room et al. 2005). Alcohol dependence is a chronic relapsing disorder involving cycles of alcohol intoxication and withdrawal. The severity of withdrawal is positively correlated to the number of intoxication and withdrawal cycles, culminating in the alcohol withdrawal syndrome with symptoms that include anxiety, insomnia, agitation, and increased susceptibility to seizures (McKeon et al. 2008). Chronic intermittent alcohol (ethanol, EtOH) exposure is thought to gradually, with each cycle of intoxication and withdrawal, decrease reward signaling while sensitizing the brain stress response system (Koob and Le Moal 2008). The resultant opposing motivational processes are hypothesized to contribute to the development of cravings and relapse. Relapse to alcohol is a critical problem in treating alcoholism, and effective treatments are yet to be found.

The nucleus accumbens (NAcc) is a key neural substrate for the rewarding actions of many drugs of abuse, including alcohol (Koob et al. 1998; Wise 2004). The NAcc is mainly (~95%) composed of GABAergic medium spiny neurons (MSNs) that project massively to the ventral pallidum, substantia nigra, and the ventral tegmental area (VTA) (Chang and Kitai 1985; Nauta et al. 1978). Optogenetic studies have demonstrated that MSNs in the NAcc specifically target GABAergic neurons in the VTA without making direct synaptic contacts with VTA dopamine neurons (Xia et al. 2011). MSNs also form functional GABAergic interconnections within the NAcc (Taverna et al. 2004). MSNs receive extensive glutamatergic inputs from prefrontal cortical areas, hippocampus, thalamus, and basolateral amygdala (Brog et al. 1993; Sesack and Grace 2010). The remaining neurons in the NAcc are subpopulations of local circuit cholinergic and GABAergic interneurons (Bennett and Bolam 1994; de Quidt and Emson 1986; Hussain et al. 1996; Vincent and Johansson 1983; Vincent et al. 1983; Zhou et al. 2002). In addition to the well-described dopaminergic input from the VTA (Beckstead et al. 1979; Dahlström and Fuxe 1964; Fallon and Moore 1978; Swanson 1982), GABAergic neurons from the VTA also send projections to the NAcc (Van Bockstaele and Pickel 1995), thus providing a reciprocal inhibitory loop to this mesolimbic circuit.

In vivo MSNs oscillate between "up" and "down" states (O'Donnell and Grace 1995). The "up" state is brought on by synaptic activation of glutamatergic receptors, which depolarizes the MSN neurons to spike firing threshold. On the basis of recordings in behaving animals it has been suggested that the "up" state is the time when NAcc neurons execute their behaviorally relevant functions (O'Donnell et al. 1999). The patterns of spike discharge are thus sculpted mainly by a combination of glutamatergic excitation, GABAergic inhibition, and modulatory influences of dopamine. Recently, we

Address for reprint requests and other correspondence: I. Spigelman, UCLA School of Dentistry, Div. of Oral Biology and Medicine, 10833 Le Conte Ave., 63-078 CHS, Los Angeles, CA 90095-1668 (e-mail: igor@ucla.edu).

0022-3077/14 Copyright © 2014 the American Physiological Society

Downloaded from on July 7, 2014

found persistent alterations in the intrinsic electrical membrane properties, K^+ currents, and glutamatergic synaptic transmission of MSNs in the NAcc core of rats following chronic intermittent ethanol (CIE) treatment (Marty and Spigelman 2012), a model of alcohol dependence (Spigelman et al. 2013). Here we studied $GABA_A$ receptor ($GABA_AR$)-mediated currents in NAcc core MSNs in CIE rats and vehicle control (CIV) rats in order to obtain a more comprehensive picture of changes in mesolimbic system signaling in alcohol dependence.

Our data indicate that CIE treatment produces alterations in the subunit composition and function of MSN $GABA_ARs$ as well as alterations in the synaptic release of GABA. Unlike the reversible plasticity of $GABA_ARs$ induced by single EtOH doses, these alterations are long-lasting and are expected to affect information transfer in the mesolimbic system in a predictable manner.

METHODS

Animals. The Institutional Animal Care and Use Committee approved all animal experiments. Male Sprague-Dawley rats (weighing 190–220 g upon arrival) were housed in the vivarium under a 12:12-h light-dark cycle and had free access to food and water. Rats were randomly assigned to two groups, a control group and a chronic intermittent EtOH (CIE) regimen group. The CIE rats for the first 5 doses received 5 g/kg of EtOH (Pharmco Products, Brookfield, CT) as a 25% (wt/vol) solution in water by oral intubation every other day, followed by 55 doses of 6 g/kg of 30% EtOH every day. The control vehicle (CIV) rats received water (20 ml/kg). These treatments were followed by 40–100 days of withdrawal prior to electrophysiological or biochemical experiments. Alternatively, rats were administered a single dose of EtOH (5 g/kg) or water (20 ml/kg) by oral intubation, followed by 1 h to 14 days of withdrawal.

Electrophysiological recordings. Transverse brain slices (400 μm thick) containing the NAcc were obtained with standard techniques. Briefly, rats were decapitated under isoflurane anesthesia and brains were quickly removed, trimmed with a razor blade, and glued to the base of a cutting chamber (Leica VT1200S) filled with cold (~4°C) artificial cerebrospinal fluid (ACSF) composed of (in mM) 125 NaCl, 2.5 KCl, 2 $CaCl_2$, 2 $MgCl_2$, 26 $NaHCO_3$, and 10 D-glucose (Sigma). The ACSF was continuously bubbled with a 95%-5% mixture of O_2 and CO_2 to ensure adequate oxygenation of slices and a pH of 7.4. Patch electrode filling solutions contained (in mM) 135 cesium gluconate, 2 $MgCl_2$, 1 $CaCl_2$, 11 ethylene glycol-bis(β-aminoethyl ether)-*N,N,N′,N′*-tetraacetic acid (EGTA), 10 HEPES, 2 ATP-K_2, and 0.2 GTP-Na_2; pH adjusted to 7.25 with CsOH. Patch electrode and probe assembly targeting the region of interest were advanced with a four-axis motorized manipulator (MX7600, Siskiyou, Grants Pass, OR) and controller (MC1000e, Siskiyou) with the aid of a dissecting microscope (×7–45, SZ61, Olympus). Whole cell patch-clamp recordings were obtained with a Multiclamp 700B amplifier and a Digidata 1440A A/D converter (Molecular Devices, Sunnyvale, CA) from cells in the NAcc core region during perfusion (1 ml/min) with oxygenated ACSF at 34 ± 0.5°C. Most cells were putatively identified as MSNs within 30 s of membrane breakthrough by the presence of a characteristic delay in action potential generation with depolarizing current pulses (Marty and Spigelman 2012); those that did not possess these characteristics were discarded. Next, $GABA_AR$-mediated currents were separated pharmacologically by application of TTX (0.5 μM), CNQX (10 μM), APV (40 μM), and CGP54626 (1 μM) in the ACSF. Cells were subsequently voltage-clamped at 0 mV, and recordings began at least 10 min after membrane breakthrough to ensure adequate dialysis by intrapipette contents. EtOH (10–100 mM), diazepam (DZ, 0.3 μM), and Ro15-4513 (0.3 μM) were applied after appropriate dilution in the ACSF.

Detection and analysis of miniature inhibitory postsynaptic currents and tonic currents. The recordings were low-pass filtered (Clampfit software, Molecular Devices) at 2 kHz and analyzed with the aid of the Mini Analysis Program (Synaptosoft, Fort Lee, NJ). Miniature inhibitory postsynaptic currents (mIPSCs) were detected with threshold criteria of 5-pA amplitude and 20-fC charge transfer. Frequency of mIPSCs was determined from all automatically detected events in a given 100-s recording period. Tonic current magnitudes were obtained from the mean baseline current of a given recording period. For kinetic analysis of mIPSCs, only single events with a stable baseline, sharp rising phase, and exponential decay were chosen. Double and multiple-peak mIPSCs were excluded. The mIPSC kinetics were obtained from analysis of the averaged chosen single events (>120 events/200-s recording period) aligned with half rise time in each cell. Decay time constants were obtained by fitting a double-exponential equation to the falling phase of the averaged mIPSCs of the form $I(t) = I_f \times \exp(-t/\tau_f) + I_s \times \exp(-t/\tau_s)$, where I_f and I_s are the amplitudes of the fast and slow decay components and τ_f and τ_s are their respective decay time constants used to fit the data. To compare decay times, we used a weighted mean decay time constant: $\tau_w = [I_f/(I_f + I_s)] \times t_f + [I_s/(I_f + I_s)] \times t_s$. Histograms of rise time and other mIPSC kinetics were built with the data analysis and graphing software Origin (V7, OriginLab, Northampton, MA). The histograms were fitted with the multipeaks (Gaussian) fitting tool in Origin.

Membrane preparation and Western blotting. NAcc sections were microdissected from individual 400-μm-thick brain sections. Both core and shell regions of the NAcc were included because previous studies did not detect any major differences in the distribution of $GABA_AR$ subunits between these regions (Pirker et al. 2000). Sections were incubated in a small-volume chamber with or without the protein cross-linking reagent bis(sulfosuccinimidyl)suberate (BS^3) in ACSF at 4°C according to Grosshans et al. (2002). BS^3 is bifunctional and cross-links all proteins exposed to the medium, i.e., cell surface proteins. These large complexes are retained at the top of the gel; thus the band of protein at the identified molecular weight corresponds to that fraction that is intracellular only. The difference between that value and the amount from an equivalent adjacent slice, untreated, and thus total, represents the surface pool. After incubation of NAcc sections in the absence (total) or presence (intracellular) of BS^3, sections were washed three times with Tris wash buffer (pH 7.6) to wash away free BS^3. The washed sections were homogenized in a buffer composed of 1% SDS, 1 mM EDTA, and 10 mM Tris, pH 8.0. Protein content was measured by the Bio-Rad D_C protein assay system. Protein aliquots (15–40 μg) from samples were separated on 10% SDS-polyacrylamide gel electrophoresis under reducing conditions with the Bio-Rad Mini-Protean 3 Cell system. Proteins were transferred to PVDF membranes (Immun-Blot PVDF membrane, 0.2 mm, Bio-Rad) with Mini-Protean 3 Trans-Blot (Bio-Rad) or the Trans-Blot SD semidry transfer cell system (Bio-Rad). Blots were probed with anti-peptide α1 (proprietary N-terminus synthetic antigen, Novus Biologicals, Littleton, CO), α2 (aa322–357), α3 (aa459–467), α4 (aa379–421), α5 (aa337–388), γ2 (aa319–366), or δ (aa331–430, Santa Cruz Biotechnology) antibodies (all at 1 mg/ml), followed by HRP-conjugated anti-rabbit (Millipore, Billerica, MA), and bands were detected with the Amersham ECL Plus detection kit (GE Healthcare Life Sciences, Piscataway, NJ), apposed to X-ray film under nonsaturating conditions or digitally captured with an LAS-3000 imager (Fujifilm, Tokyo, Japan). W. Sieghart and colleagues (Medical University of Vienna, Vienna, Austria) kindly provided the α1, α2, α3, α4, α5, and γ2 $GABA_AR$ subunit antibodies. These antibodies have been previously extensively verified by various methods including immunoprecipitation, Western blotting, and immunocytochemistry (Mossier et al. 1994; Zezula et al. 1991; Zimprich et al. 1991). A β-actin antibody (aa1–100; Abcam, Cambridge, MA) was used as a loading control in all experiments. Bands from different samples corresponding to the appropriate subunit were analyzed and absorbance

Downloaded from on July 7, 2014

values compared by densitometry using either C.IMAGING analysis systems (Complix, Cranberry Township, PA) or ImageJ (National Institutes of Health, Bethesda, MD). Group differences were evaluated by *t*-test. $P < 0.05$ was considered statistically significant.

Histology. CIV ($n = 4$) and CIE ($n = 4$) rats were anesthetized with pentobarbital (100 mg/kg ip) and each perfused transcardially first with ~200 ml of cold NaCl (0.8%) solution containing dextrose (0.4%), sucrose (0.8%), $CaCl_2$ (0.023%), and sodium cacodylate (0.034%) followed by ~300 ml of a fixative solution composed of paraformaldehyde (4%), sucrose (4%), and sodium cacodylate (1.4%). Brains were postfixed overnight in a sodium cacodylate (1.4%) storage buffer. Subsequently, brains were embedded with the MultiBrain Technology (NeuroScience Associates, Knoxville, TN) and freeze-sectioned at 60 μm in the coronal plane, every sixth section (360-μm intervals) was processed for NeuN immunohistochemistry to reveal the neuron-specific marker protein and counterstained with Neutral Red, and individual sections were mounted on slides and coverslipped.

Stereology. NeuN-stained cell bodies were quantitatively and qualitatively evaluated for both neuronal number and cell body volume. Estimates were performed ipsilaterally. Brain area was defined anatomically by atlas and the agreement of two investigators (Paxinos and Watson 1998). Every eighth section of NAcc was selected from a random initial sort to ensure random overall sampling. Additionally, the MultiBrain Technology used for the histological procedure ensures that brains embedded in gelatin prior to sectioning possess enough variance to provide a random and unbiased sampling of each of a potential 16 brain sections on each slide (although only 8 were used for this study). The optical fractionator method and the Stereologer software package (Mouton 2000) were used to count NeuN-stained cells. The study used a Nikon Eclipse 80i microscope, linked to a Sony 3CCD Color Digital Video Camera, which operated an Advanced Scientific Instrumentation MS-2000 motorized stage input into a Dell Precision 650 Server and a high-resolution plasma monitor.

The areas of interest were defined with a ×4/1.3 aperture dry lenses, and the stereology was performed at high magnification with ×100/1.4 aperture oil immersion lenses (yielding ×3,600) that allow for clear visualization of the nucleolus and precise definition of the cell walls. When the areas of interest were identified, areas were precisely outlined and checked against an atlas (Paxinos and Watson 1998). The inclusion grid was randomly applied by the software, and high-resolution microscopy was then used to count NeuN-stained neurons. Additionally, the nucleator method was performed on each counted neuron to assess cell body volume.

Statistical analysis. The investigators performing the recordings, mIPSC, Western blot, and stereology analysis were blind to the treatment (CIV or CIE) that the rats received. All summary values are presented as means ± SE. Group differences were evaluated by unpaired Student's *t*-test, one-way analysis of variance (ANOVA), two-way ANOVA, or two-way repeated-measures (RM) ANOVA, where appropriate. $P < 0.05$ was considered statistically significant.

RESULTS

CIE-induced switch in EtOH responsiveness from extrasynaptic to synaptic $GABA_ARs$. After putative identification of NAcc neurons as MSNs in current-clamp recordings, we switched to voltage clamp and recorded $GABA_AR$ currents during pharmacological blockade of ionotropic glutamate receptors, $GABA_BRs$, and voltage-gated sodium channels. Under these recording conditions $GABA_AR$ currents could be separated into two components: a nondesensitizing tonic current (I_{tonic}) and phasic mIPSCs, which are known to be mediated by extrasynaptic and synaptic $GABA_AR$ activation, respectively (Mody and Pearce 2004). Acute application of EtOH (10–100 mM) in MSN recordings from CIV-treated rats preferentially potentiated the picrotoxin-sensitive I_{tonic}, whereas the charge transfer (area) of phasic mIPSCs was unaffected by the same concentrations of applied EtOH (Fig. 1). In contrast, in MSN recordings from CIE-treated rats, it was the mIPSC area that was significantly potentiated by EtOH (50–100 mM), whereas the I_{tonic} was completely insensitive to potentiation by EtOH (10–100 mM). The increases in mIPSC charge transfer resulted primarily from significant increases in decay time constants (τ_1 and τ_2) without significant increases in mIPSC amplitude (Fig. 1*C*). There was a trend toward increased frequency of mIPSCs in MSNs from both CIV (~7%, $P = 0.13$) and CIE (~9%, $P = 0.08$) rats, but only by 10 mM EtOH. The rise time (10–90%) of mIPSCs was also not significantly affected by acute EtOH (10–100 mM) application in MSNs from CIV or CIE rats (Fig. 1*C*). In the absence of significant effects of acute EtOH on mIPSC frequency, our data are consistent with CIE-induced increases in responsiveness of synaptic $GABA_ARs$ and decreases in responsiveness of extrasynaptic $GABA_ARs$ to acute EtOH.

CIE-induced switch in Ro15-4513 responsiveness of extrasynaptic and synaptic $GABA_ARs$. Previous studies in other brain regions suggested that the EtOH-sensitive extrasynaptic $GABA_ARs$ of CIV rats may be composed of $\alpha4\beta\delta$ subunit combinations (Sundstrom-Poromaa et al. 2002; Wallner et al. 2003), which may be replaced by synaptic apparently EtOH-sensitive $\alpha4\beta\gamma2$ $GABA_ARs$ after CIE treatment (Liang et al. 2007). To explore this possibility we examined the effect of CIE treatment on responses to Ro15-4513, a partial inverse agonist at the benzodiazepine (BZ) site of $\alpha1$- and $\alpha2$-containing $GABA_ARs$, which was also shown to bind with high affinity at $\alpha4$-containing $GABA_ARs$ (Knoflach et al. 1996). Importantly, Ro15-4513 has agonist activity at $\alpha4\beta3\gamma2$ $GABA_ARs$ but does not modulate $\alpha4\beta3\delta$ $GABA_ARs$ (Brown et al. 2002). Application of Ro15-4513 (0.3 μM) preferentially potentiated I_{tonic} (~80%) compared with mIPSCs (~18%) in MSN recordings from CIV rats (Fig. 2, *A* and *B*), suggesting a significant contribution of $\alpha4\beta\gamma2$ $GABA_ARs$ to the tonic inhibitory current. In contrast, similar applications of Ro15-4513 in recordings from CIE rat MSNs preferentially potentiated mIPSCs (~40%) compared with I_{tonic} (~18%) (Fig. 2, *A* and *B*). The potentiation of mIPSCs by Ro15-4513 was mainly due to the slowing of the rise and decay rates of mIPSCs (Fig. 2*C*). Ro15-4513 application had no effect on the frequency of mIPSCs in MSNs from either CIV or CIE rats (Fig. 2*C*). These data provided further pharmacological evidence for CIE-induced increases in contribution of $\alpha4\beta\gamma2$ $GABA_ARs$ to synaptic currents.

CIE-induced decreases in diazepam responsiveness of extrasynaptic and synaptic $GABA_ARs$. To provide additional pharmacological evidence for the specificity of CIE-induced $GABA_AR$ subunit plasticity, we tested mIPSC and I_{tonic} responsiveness to acute DZ (0.3 μM) application. Since DZ has no agonist activity at $\alpha4$ (or $\alpha6$)-containing $GABA_ARs$ but potentiates other $\alpha x\beta\gamma2$ $GABA_ARs$ (Möhler et al. 2000), we expected that increases in $\alpha4$-containing $GABA_ARs$ would result in diminished potentiation of currents mediated by either synaptic or extrasynaptic $GABA_ARs$. In NAcc slices from CIV rats, DZ increased the magnitude of I_{tonic} and increased the charge transfer of mIPSCs primarily by prolonging their decay, although there was also a small (~5%) but significant increase in mIPSC amplitude (Fig. 3). In contrast, in MSN recordings

Downloaded from on July 7, 2014

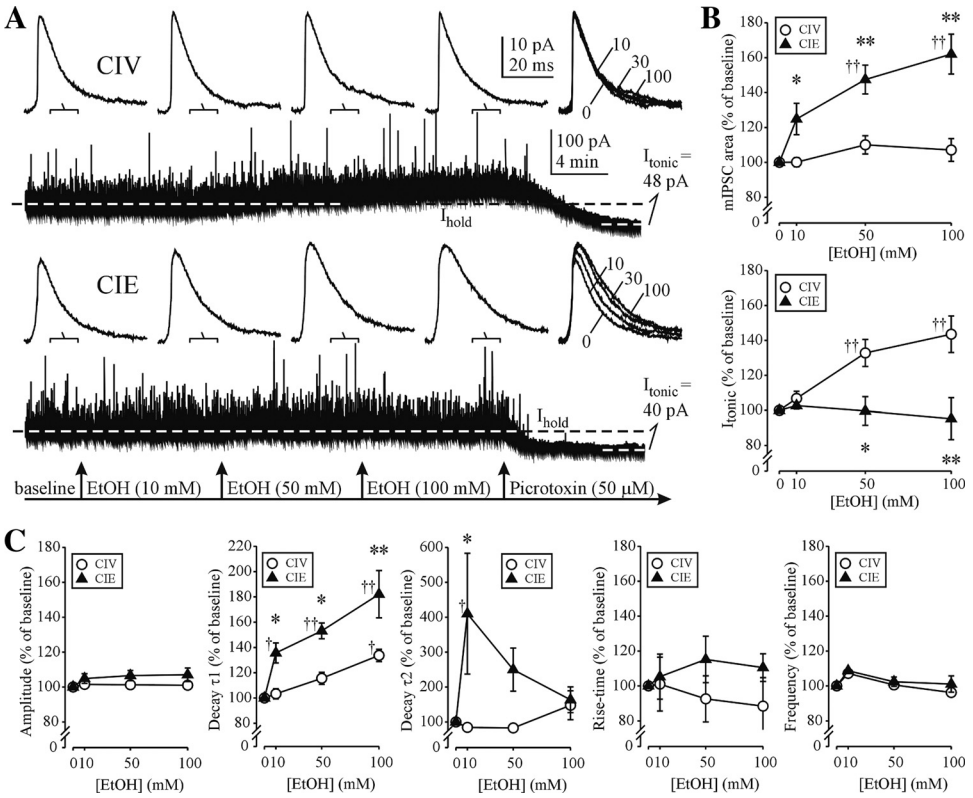

Fig. 1. Decreased potentiation of the nucleus accumbens (NAcc) GABA type A receptor (GABA$_A$R)-mediated tonic current (I_{tonic}) and enhanced potentiation of miniature inhibitory postsynaptic currents (mIPSCs) by acute EtOH after chronic intermittent EtOH (CIE) treatment and >40 days of withdrawal. *A*: examples of individual NAcc neuron recordings from vehicle-treated (CIV, *top*) and CIE-treated (*bottom*) rats. The holding current (I_{hold}) needed to clamp the voltage at 0 mV before EtOH application is indicated by a dashed line. In a control recording, the kinetics of mIPSCs (*top* traces) averaged over the indicated 100-s periods during continuous recordings (*bottom* trace) are unaffected by 100 mM EtOH, whereas I_{hold} is visibly potentiated. Subsequent application of picrotoxin (50 μM) reveals the I_{tonic} component. After CIE treatment there is a loss of I_{tonic} potentiation (*bottom* trace), whereas mIPSCs are visibly potentiated even by 10 mM EtOH. *B*, *top*: mIPSCs from vehicle-treated rats are insensitive to EtOH, whereas after CIE treatment mIPSCs are significantly potentiated by 50–100 mM EtOH [treatment: $F(1,35) = 58.3$, $P < 0.001$; EtOH concentration ([EtOH]): $F(3,35) = 11.62$, $P < 0.001$; treatment × [EtOH] interaction: $F(3,35) = 6.28$, $P = 0.003$]. *Bottom*: I_{tonic} is significantly potentiated by acute application of 50 and 100 mM EtOH in vehicle- but not CIE-treated rats [treatment: $F(1,35) = 7.8$, $P = 0.027$; [EtOH]: $F(3,35) = 6.04$, $P = 0.004$; treatment × [EtOH] interaction: $F(3,35) = 9.57$, $P < 0.001$]. Each point represents a mean ± SE value from 4 or 5 neurons (2 or 3 rats/group). *C*: summary graphs of EtOH-induced changes in various mIPSC kinetic parameters. Decay τ_1: treatment: $F(1,35) = 29.2$, $P = 0.001$; [EtOH]: $F(3,35) = 23.2$, $P < 0.001$; treatment × [EtOH] interaction: $F(3,35) = 4.2$, $P = 0.018$. Decay τ_2: treatment: $F(1,35) = 6.45$, $P = 0.039$; [EtOH]: $F(3,35) = 2.25$, $P = 0.11$; treatment × [EtOH] interaction: $F(3,35) = 3.54$, $P = 0.032$. **$P < 0.001$, *$P < 0.05$ vs. CIV group; ††$P < 0.001$, †$P < 0.01$ vs. pre-EtOH baseline value [2-way repeated-measures (RM) ANOVA with Holm-Sidak post hoc].

from CIE-treated rats DZ application had no significant effect on either I_{tonic} or mIPSCs. We also observed a small (~12%) but significant increase in mIPSC frequency by DZ in recordings from CIV but not CIE rats (Fig. 3*C*).

CIE-induced alterations in mIPSC kinetics. Since the subunit composition of GABA$_A$Rs affects both their pharmacology and kinetics, we next compared the kinetic properties of mIPSCs and the magnitude of I_{tonic} between MSNs from CIV and CIE rats before application of GABA$_A$R modulators. Table 1 illustrates that the averaged mIPSCs obtained from all recordings in MSNs from CIE rats had significantly reduced amplitude, increased rise time, and a small, but significant, decrease in mIPSC frequency compared with recordings from CIV rats. The average basal magnitude of I_{tonic}, which ranged from 19.2 to 67.0 pA in CIV and from 15.0 to 47.1 pA in CIE recordings, was similar in the two groups. However, because of the low power (0.05) of the performed statistical test, these negative findings should be interpreted cautiously. The observed changes in amplitude and rise time of mIPSCs are consistent with possible alterations in the subunit composition of postsynaptic GABA$_A$Rs. However, alterations in mIPSC frequency are usually consistent with changes in presynaptic transmitter release or the numbers of active synapses (Korn and Faber 1991).

CIE-induced decreases in frequency of fast-rising mIPSCs. The large increases in average mIPSC rise time (10–90%) and decreases in mIPSC amplitudes were quite different from our previous experience in hippocampal recordings from CIE rats (Cagetti et al. 2003; Liang et al. 2006). Therefore, we performed separate histogram analyses of mIPSC rise times and amplitudes comparing their distributions between recordings from all CIV and CIE MSNs. A histogram analysis of mIPSC rise times revealed a significant decrease in the proportion of fast-rising events in MSNs from CIE rats compared with CIV control rats (Fig. 4). Furthermore, the mIPSC amplitudes were, as expected, larger for mIPSCs with faster rise times in both CIV and CIE rats (not shown). These data were consistent with preferential decreases in fast-rising, larger-amplitude mIPSCs in MSNs from CIE rats.

CIE treatment does not alter NAcc volume, neuronal numbers, or neuronal cell body volume. To determine whether the functional alterations in GABAergic neurotransmission could

Downloaded from on July 7, 2014

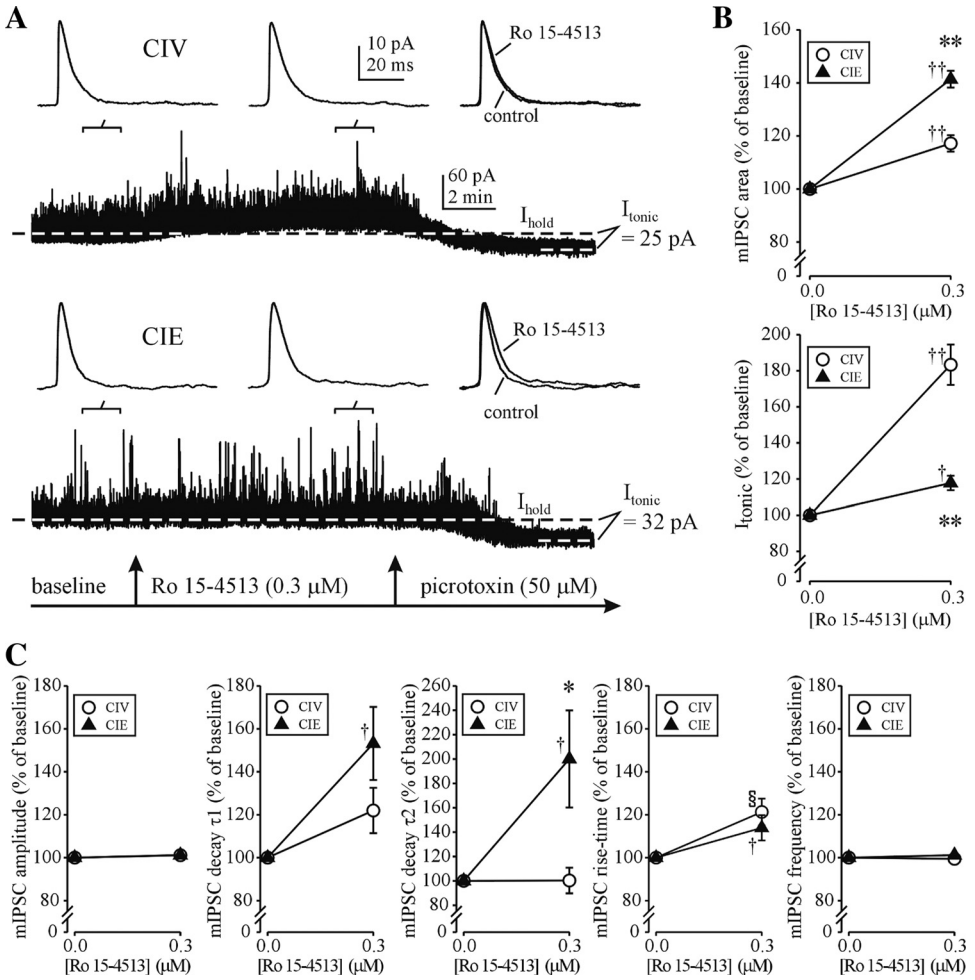

Fig. 2. Decreased potentiation of the NAcc GABA$_A$R-mediated tonic current and enhanced potentiation of mIPSCs by Ro15-4513 after CIE treatment and >40 days of withdrawal. *A*: examples of individual NAcc neuron recordings from CIV-treated (*top*) and CIE-treated (*bottom*) rats. Note the loss of Ro15-4513 (0.3 μM) potentiation of both I_{tonic} and mIPSCs from CIE rats. *B*: mIPSCs (*top*) are potentiated by Ro15-4513 in CIE but not CIV rats [treatment: $F(1,21) = 28.9$, $P < 0.001$; [Ro15-4513]: $F(1,21) = 169.7$, $P < 0.001$; treatment × [Ro 15–4513] interaction: $F(1,21) = 28.9$, $P < 0.001$], while I_{tonic} (*bottom*) is potentiated in CIV but not CIE rats [treatment: $F(1,21) = 35.3$, $P < 0.001$; [Ro15-4513]: $F(1,21) = 84.1$, $P < 0.001$; treatment × [Ro15-4513] interaction: $F(1,21) = 35.3$, $P < 0.001$]. *C*: summary graphs of [Ro15-4513]-induced changes in various mIPSC kinetic parameters. Decay τ_1: treatment: $F(1,21) = 2.2$, $P = 0.16$; [Ro15-4513]: $F(1,21) = 12.7$, $P = 0.002$; treatment × [Ro15-4513] interaction: $F(1,21) = 2.2$, $P = 0.16$. Decay τ_2: treatment: $F(1,21) = 4.91$, $P = 0.04$; [Ro15-4513]: $F(1,21) = 4.96$, $P = 0.039$; treatment × [Ro15-4513] interaction: $F(1,21) = 4.91$, $P = 0.04$. Rise time: treatment: $F(1,21) = 0.73$, $P = 0.4$; [Ro15-4513]: $F(1,21) = 16.7$, $P < 0.001$; treatment × [Ro15-4513] interaction: $F(1,21) = 0.73$, $P = 0.4$. Each point represents a mean ± SE value from 6 or 7 neurons (2–4 rats/group). $^{**}P < 0.001$, $^{*}P < 0.05$ vs. CIV group; $^{††}P < 0.001$, $^{†}P < 0.01$, $^{§}P < 0.05$ vs. pre-Ro15-4513 baseline value (2-way ANOVA with Holm-Sidak post hoc).

result from possible neurodegenerative changes within the NAcc of CIE rats, we performed unbiased stereological analysis of NeuN-stained NAcc neurons by investigators blinded to the nature of treatments received by the rats. This analysis revealed a lack of any significant changes in NAcc volume, neuronal numbers, or neuronal cell body volume in sections from CIE rats compared with their CIV controls (Fig. 5). However, because of the low power (0.15) of the performed statistical test, these negative findings should be interpreted cautiously.

CIE-induced long-lasting changes in surface GABA$_A$R subunit levels. To study the biochemical correlates of functional GABA$_A$R changes, we compared Western blots from microdissected NAcc slices of CIE- and CIV-treated rats incubated with or without the membrane-impermeant cross-linking reagent BS^3. In this way, we were able to identify the intracellular and, indirectly, the cell surface pools of GABA$_A$R subunits (Grosshans et al. 2002). Cell surface proteins form high-molecular-weight aggregates with BS^3, such that they remain at the top of the gel (Grosshans et al. 2002; Liang et al. 2007). However, intracellular proteins are not accessed by the membrane-impermeant reagent and thus can be quantified through Western blot analysis. Subtraction of the intracellular protein from the total protein estimates the cell surface protein content. Such analysis revealed significant decreases in the surface levels of α1 and δ subunits in the NAcc of CIE rats (Fig. 6). In contrast, the surface levels of α4, α5, and γ2 subunits were significantly increased, while those of α2 and α3 GABA$_A$R subunits were unchanged in NAcc of rats after CIE treatment and >40 days of withdrawal (Fig. 6).

Single-dose EtOH-induced reversible changes in surface GABA$_A$R subunit levels. To explore the mechanisms of EtOH-induced GABA$_A$R plasticity, we studied the time dependence of changes in the surface levels of select GABA$_A$R subunits in the NAcc in response to a single intoxicating dose of EtOH (5 g/kg, gavage), which results in a peak plasma EtOH concentration ([EtOH]) of ~275 mg/dl (Liang et al. 2007). We chose to focus on the 1 h, 2 days, and 14 days post-EtOH time points because previous studies in the hippocampus at these time points revealed EtOH-induced rapid internalization of α4βδ extrasynaptic GABA$_A$Rs and subsequent preferential expression of α4βγ2 synaptic GABA$_A$Rs (Liang et al. 2007). Analysis of NAcc Western blots revealed a clear increase in the intracellular α4 subunit protein fraction at 1 h after EtOH administration (Fig. 7). These increases occurred at the expense of the cell surface α4 subunit content because total content was unchanged at 1 h after EtOH intoxication (not shown). At 2 days after EtOH there was a large increase in the surface α4 subunit protein, which gradually returned to control levels at 14 days (Fig. 7). In contrast, intracellular and total α1 subunit content were unchanged at 1 h after EtOH, but at 2 days after single-dose EtOH both intracellular and surface content were significantly reduced, consistent with the persistent decrease in α1 seen in CIE, with recovery to control levels

Downloaded from on July 7, 2014

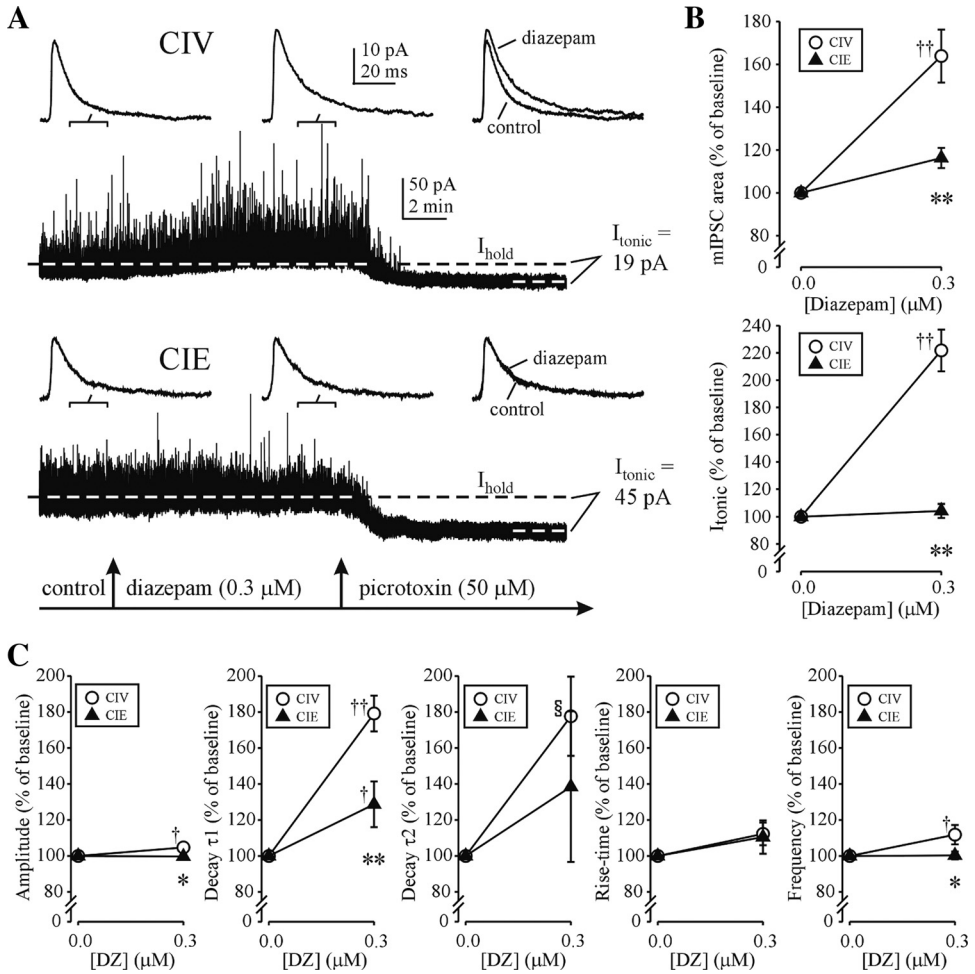

Fig. 3. Decreased potentiation of NAcc GABA$_A$R-mediated tonic and phasic currents by diazepam (DZ) after CIE treatment and >40 days of withdrawal. *A*: examples of individual NAcc neuron recordings from CIV-treated (*top*) and CIE-treated (*bottom*) rats. Note the loss of DZ (0.3 μM) potentiation of both I_{tonic} and mIPSCs from CIE rats. *B*: mIPSCs (*top*) and I_{tonic} (*bottom*) are potentiated by DZ in CIV but not CIE rats [mIPSC area: treatment: $F(1,25) = 14.6$, $P < 0.001$; [DZ]: $F(1,25) = 41.5$, $P < 0.001$; treatment × [DZ] interaction: $F(1,25) = 14.6$, $P < 0.001$; I_{tonic}: treatment: $F(1,25) = 60.6$, $P < 0.001$; [DZ]: $F(1,25) = 69.6$, $P < 0.001$; treatment × [DZ] interaction: $F(1,25) = 60.6$, $P < 0.001$]. *C*: summary graphs of DZ-induced changes in various mIPSC kinetic parameters. Amplitude: treatment: $F(1,25) = 5.47$, $P = 0.029$; [DZ]: $F(1,25) = 4.26$, $P = 0.051$; treatment × [DZ] interaction: $F(1,25) = 5.47$, $P = 0.029$. Decay τ_1: treatment: $F(1,25) = 9.3$, $P = 0.006$; [DZ]: $F(1,25) = 42.4$, $P < 0.001$; treatment × [DZ] interaction: $F(1,25) = 9.3$, $P = 0.006$. Decay τ_2: treatment: $F(1,25) = 0.62$, $P = 0.44$; [DZ]: $F(1,25) = 5.43$, $P = 0.029$; treatment × [DZ] interaction: $F(1,25) = 0.62$, $P = 0.44$. Frequency: treatment: $F(1,25) = 4.4$, $P = 0.048$; [DZ]: $F(1,25) = 4.9$, $P = 0.038$; treatment × [DZ] interaction: $F(1,25) = 4.4$, $P = 0.048$. Each point represents a mean ± SE value from 6 or 7 neurons (2–4 rats/group). $^{**}P < 0.001$, $^{*}P < 0.05$ between CIV and CIE groups; $^{††}P < 0.001$, $^{†}P < 0.01$, $^{§}P < 0.05$ vs. pre-DZ baseline value (2-way ANOVA with Holm-Sidak post hoc).

by 7 days (Fig. 7). We also observed that the surface α5 subunit protein at the 1 h time point was unchanged, followed by a large increase at 2 days after EtOH and recovery to control levels at the 14 day time point (Fig. 7).

The decreases in surface α4 subunit levels observed at 1 h after EtOH intoxication are consistent with rapid internalization of α4βδ extrasynaptic GABA$_A$Rs, which are sensitive to low [EtOH] (Gonzalez et al. 2012; Liang et al. 2007; Shen et al. 2011; Sundstrom-Poromaa et al. 2002; Wallner et al. 2003). Therefore, we also measured the alterations in δ subunit protein, a substantial fraction of which normally coassembles with the α4 subunits to form extrasynaptic or perisynaptic receptors (Jia et al. 2005; Liang et al. 2006; Sun et al. 2004; Wei et al. 2003, 2004). At 1 h after EtOH the cell surface δ subunit levels decreased to 37% of their vehicle controls (Fig. 8). At 2 days after EtOH, the surface δ subunit fraction remained decreased to 24% of control values, with return to control levels measured at 14 days after single-dose EtOH (Fig. 8).

Previous studies have indicated that when hippocampal δ subunit levels are diminished by EtOH treatment in vivo or in vitro, the most likely partner for the transcriptionally upregulated α4 subunit is the γ2 subunit (Liang et al. 2007; Shen et al. 2011). Therefore, we measured the changes in γ2 subunit levels in the NAcc after EtOH intoxication. At 1 h after EtOH, we could not detect significant changes in the intracellular or total γ2 subunit fractions (Fig. 8). However, at 2 days after EtOH administration there was an apparent large increase (100%) in the cell surface γ2 subunit fractions (which did not reach statistical significance because of the high variability in this data set from both groups of rats), with return to control levels measured at 14 days (Fig. 8).

Table 1. *Comparison of kinetic properties of mIPSCs and tonic current magnitude from CIV and CIE rats*

	CIV	CIE
Amplitude, pA	25.4 ± 1.1	21.4 ± 0.5*
Rise time (10–90%), ms	1.2 ± 0.2	1.9 ± 0.1*
Decay τ_1, ms	7.0 ± 0.4	7.7 ± 0.4
Decay τ_2, ms	21.3 ± 3.1	18.7 ± 1.7
τ_1 contribution to peak, %	59.6 ± 6.5	51.3 ± 7.0
Decay τ_w, ms	11.6 ± 0.9	11.9 ± 0.6
Area, fC	497.5 ± 24.7	446.5 ± 13.6
Frequency, Hz	13.5 ± 0.1	12.4 ± 0.3*
I_{tonic}, pA	34.5 ± 4.4	33.7 ± 2.5
n (cells/rats)	16/6	17/6

Values are means ± SE. mIPSC, miniature inhibitory postsynaptic current; CIE, chronic intermittent ethanol; CIV, vehicle control; τ_w, weighted time constant; I_{tonic}, tonic current. $^{*}P < 0.01$ (unpaired *t*-test) vs. CIV.

DISCUSSION

Alcohol-seeking behaviors, craving, and relapse to drinking after withdrawal are most likely dictated by long-term changes in neuronal excitability and synaptic plasticity of the brain

Downloaded from on July 7, 2014

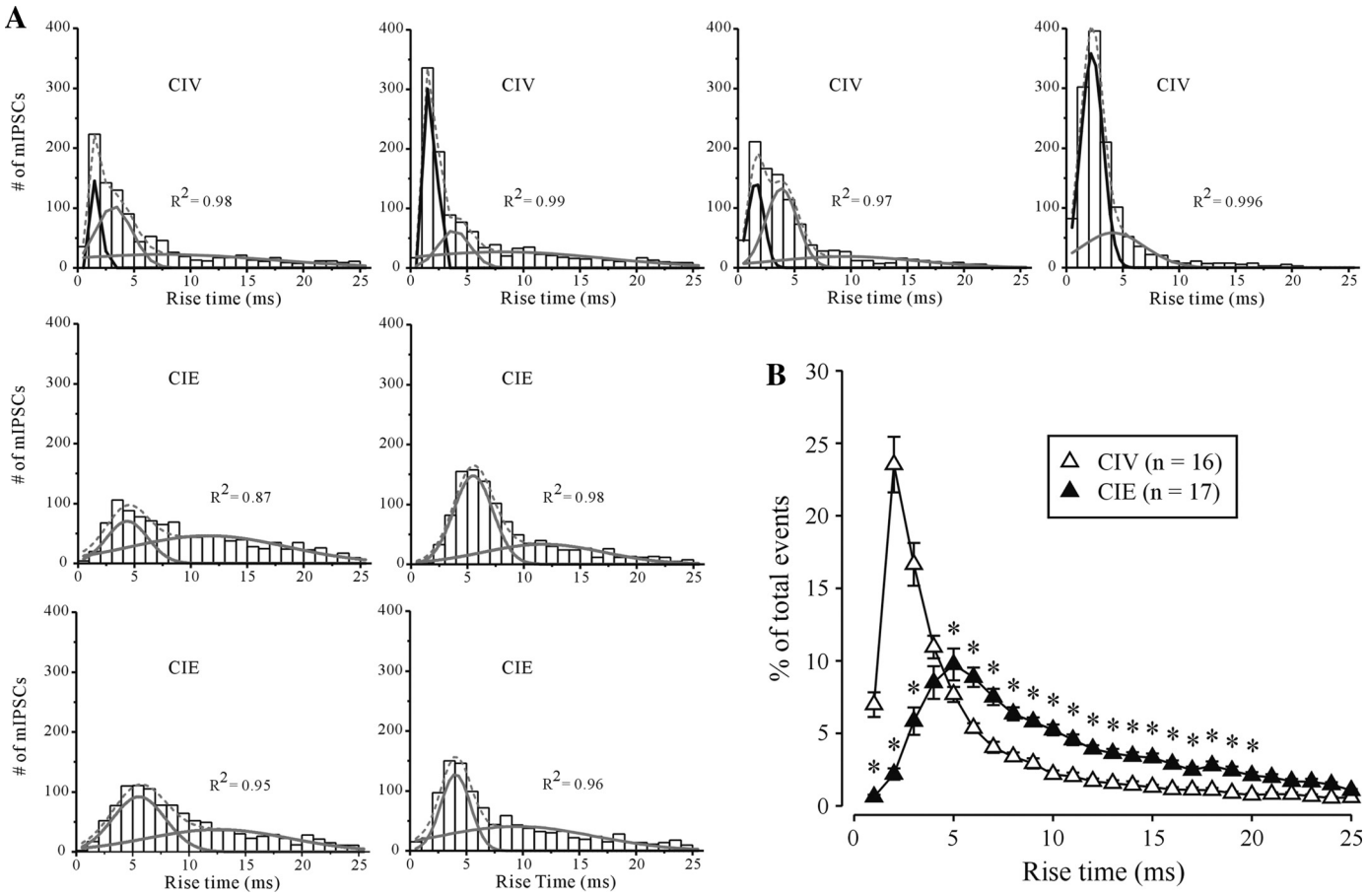

Fig. 4. Decreases in fast-rising mIPSCs after CIE treatment. *A*: histograms of mIPSC rise time (10–90%) from representative CIV and CIE recordings. The histograms were fitted to 3 or 2 populations of mIPSCs. R^2 values indicate the goodness of fit for the cumulative population curve (dashed gray curve). Note the loss of the fast-rising (1–3 ms) mIPSC population (black curve) and the remaining slow-rising mIPSC populations (gray curves) after CIE treatment. *B*: summary of mIPSC rise time histograms. Each individual histogram was first normalized by dividing the number of mIPSCs in time bins by the total number of mIPSCs in the recording, and then histograms were averaged for the CIV ($n = 16$) and CIE ($n = 17$) groups of neurons. Note the significantly larger number of mIPSCs with faster rise times recorded from CIV compared with CIE neurons [treatment: $F(1,824) = 0.505$, $P = 0.483$; rise time: $F(24,824) = 70.3$, $P < 0.001$; treatment × rise time interaction: $F(24,824) = 45.038$, $P < 0.001$; 2-way RM ANOVA, with Holm-Sidak post hoc]. Each point represents a mean ± SE value from 16 or 17 neurons (6 rats/group). *$P < 0.05$ CIV vs. CIE at specified points.

reward and stress systems (Koob and Le Moal 2008). Here we demonstrate profound plasticity of GABAergic inhibitory neurotransmission in the MSNs of NAcc, a key neural substrate for the rewarding actions of many drugs of abuse, including alcohol. This plasticity involves both presynaptic and postsynaptic elements. The observed decreases in the basal frequency of GABAergic mIPSCs from CIE rats are consistent with decreases in vesicular GABA release or decreases in the number of active GABA release sites (Korn and Faber 1991). Histograms of mIPSC rise times were also consistent with preferential decreases in frequencies of mIPSCs with fast rise times and larger amplitudes. Decreases in the number of GABA release sites could result from the degeneration of GABAergic neurons and their associated synaptic terminals on the NAcc MSNs. Fast-spiking (FS) GABAergic interneurons preferentially form synapses on the cell bodies of MSNs, while the GABAergic MSNs innervate mainly the dendritic regions of neighboring MSNs (Koos et al. 2004; Tepper et al. 2008). Unbiased stereological analysis of neurons in the NAcc failed to detect any decreases in neuronal numbers or their volumes that would indicate neurodegenerative changes in the NAcc of CIE rats. One possibility is that neurodegenerative changes may be limited to only a small population of FS interneurons, which constitute <5% of neurons in the NAcc and therefore are not detectable by our stereological analysis. Future studies focusing on parvalbumin-positive FS interneurons might be useful in that regard. Another possibility is that neurodegenerative changes are limited only to GABAergic neurons with cell

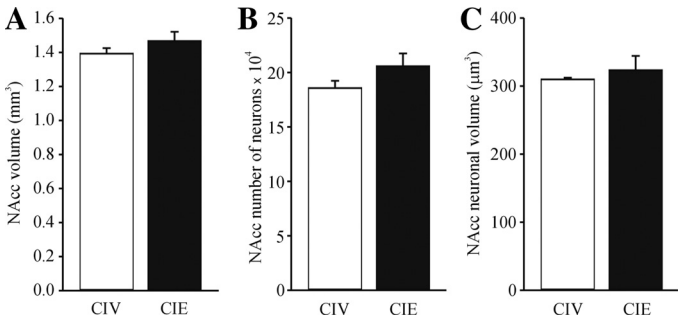

Fig. 5. Lack of changes in NAcc volume and neuronal counts after CIE treatment. *A*: summary graph comparing unbiased stereological measures of NAcc volume in CIV ($n = 4$) and CIE ($n = 4$) rats. *B*: summary graph comparing NAcc neuronal counts in CIE and CIE rats. *C*: summary graph comparing NAcc neuronal volumes in CIV and CIE rats. Note the absence of significant changes in all 3 measured parameters (unpaired *t*-test).

Downloaded from on July 7, 2014

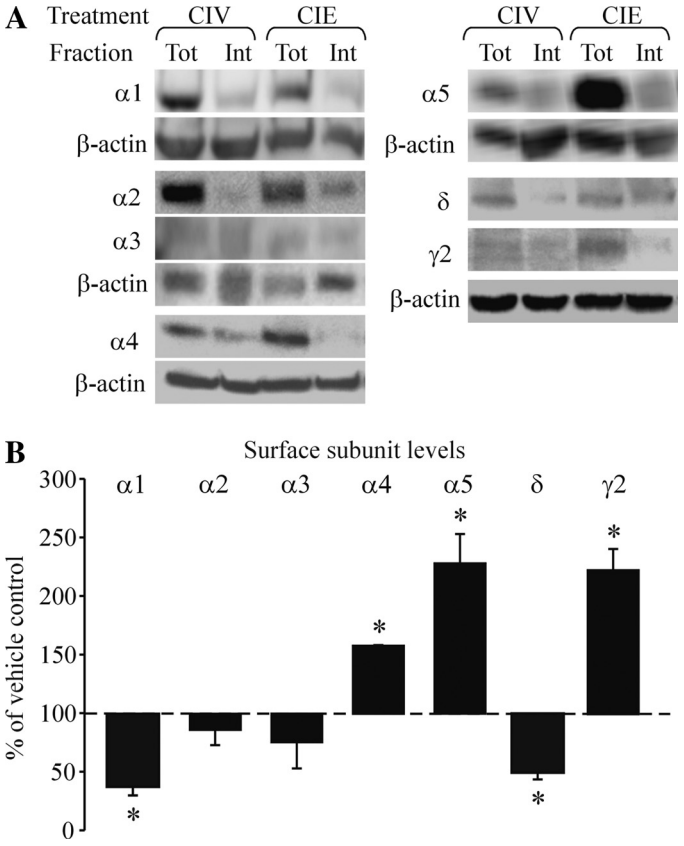

Fig. 6. Altered surface GABA$_A$R subunit levels in the NAcc of CIE rats. *A*: examples of gels from the microdissected NAcc region incubated with ACSF (Tot) or with the bis(sulfosuccinimidyl)suberate (BS^3) cross-linking reagent (Int). BS^3-linked cell surface proteins are present as high-molecular-weight aggregates that do not reliably enter the gel. In contrast, gel migration of the intracellular protein β-actin is unaffected. After each "Int" band intensity is normalized to its β-actin control, the difference between that value and the amount from an equivalent "Tot" adjacent slice represents the surface pool. *B*: summary graph of changes in cell surface GABA$_A$R subunits after CIE treatment relative to CIV controls (dashed line). Data are means ± SE from CIV or CIE treatments (n = 4–6 rats/treatment). *$P < 0.05$ (unpaired t-test) compared with CIV controls.

bodies outside the NAcc, such as the reciprocal GABAergic pathway from the VTA (Van Bockstaele and Pickel 1995). However, recent optogenetic studies revealed that this projection, at least in mice, forms synapses almost exclusively on a very small population of cholinergic interneurons in the NAcc (Brown et al. 2012), which was not examined in our recordings. Alternatively, decreases in GABA release in the NAcc of CIE-treated rats may be mediated by active mechanisms that do not involve neurodegeneration-induced decreases in the numbers of GABAergic synaptic release sites.

Long-lasting alterations in the MSNs of CIE rats also involved postsynaptic GABA$_A$R function. The pharmacological responsiveness of postsynaptic GABA$_A$Rs was altered such that the sensitivity of I_{tonic}, mediated by extrasynaptic GABA$_A$Rs, to EtOH, Ro15-4513, and DZ was greatly reduced. In contrast, sensitivity of mIPSCs in MSNs from CIE rats to both EtOH and Ro15-4513 was enhanced, while DZ sensitivity was lost. Notably, acute EtOH application did not alter action potential-independent mIPSC frequency in CIV or CIE rats, in contrast to observations in central amygdala, where EtOH application does increase mIPSC frequency (Nie et al. 2009; Roberto et al.

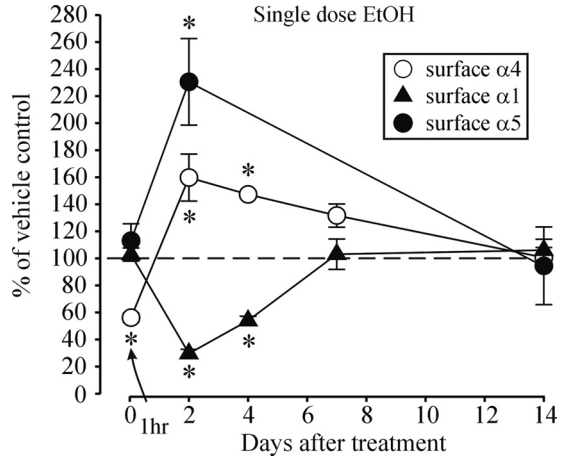

Fig. 7. Reversible changes in α1, α4, and α5 subunit proteins in microdissected NAcc after single EtOH dosing: summary graph of changes in cell surface α1, α4, and α5 subunit content at various time points after single-dose EtOH (5 g/kg, gavage) relative to vehicle-treated controls (dashed line). Data are means ± SE from vehicle or single-dose EtOH treatments (n = 4 or 5 rats/treatment). *$P < 0.05$ (unpaired t-test) compared with vehicle-treated controls.

2003). Therefore EtOH-induced potentiation of mIPSCs in NAcc MSNs is mediated by postsynaptic mechanisms rather than by increased presynaptic release of GABA. We previously reported analogous pharmacological changes in recordings from CA1 pyramidal and dentate granule neurons from CIE rats (Liang et al. 2006, 2007). Such changes in MSNs of CIE rats are consistent with cell location-specific alterations in the relative abundance and subunit composition of GABA$_A$Rs. Thus we hypothesized that decreases in I_{tonic} sensitivity to EtOH and Ro15-4513 involve decreased abundance of extrasynaptic $\alpha4\beta\delta$ GABA$_A$Rs, while decreases in DZ sensitivity were hypothesized to involve decreases in $\alpha1\beta\gamma2$ GABA$_A$Rs and increases in α4-containing GABA$_A$Rs at both synaptic and extrasynaptic sites.

The use of Western blot techniques permitted us to relate changes in the function of GABA$_A$Rs to changes in the relative surface levels of individual GABA$_A$R subunits. Consistent with the above hypothesis, we show significant decreases in surface

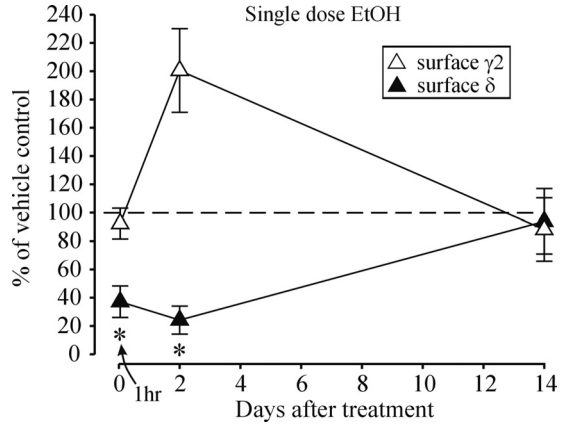

Fig. 8. Reversible changes in δ and γ2 subunit proteins in microdissected NAcc at 1 h, 2 days, and 2 wk after single EtOH dosing: summary graph of changes in cell surface δ and γ2 subunit content after single-dose EtOH relative to vehicle-treated controls (dashed line). Data are means ± SE from vehicle or single-dose EtOH treatments (n = 4–8 rats/treatment). *$P < 0.05$ (unpaired t-test) compared with vehicle-treated controls.

Downloaded from on July 7, 2014

levels of α1 and δ subunits, unaltered α2 and α3 subunit levels, and significant increases in α4, α5, and γ2 subunit levels in the NAcc of CIE rats. These changes are remarkably similar to those previously observed in the hippocampus of CIE rats (Cagetti et al. 2003; Liang et al. 2007). Analogous alterations in the α1, α4, and γ2 subunit levels were reported in the basolateral amygdala of rats after CIE treatment and withdrawal (Diaz et al. 2011). One important exception is the increase in α5 subunit levels in the NAcc, which was not observed in the hippocampus of CIE rats. Previous studies revealed an important role of α5 subunits in mediating I_{tonic} in murine striatal MSNs (Ade et al. 2008; Janssen et al. 2009). These studies also revealed, using transgenic mice, that δ subunits are not necessary for the activation of I_{tonic} by α5-containing GABA$_A$Rs (Janssen et al. 2009). Taken together, these observations suggest that CIE treatment leads to reductions in extrasynaptic (EtOH sensitive, DZ insensitive) $\alpha4\beta3\delta$ and reductions in both synaptic and extrasynaptic (EtOH insensitive, DZ sensitive) $\alpha1\beta\gamma2$ GABA$_A$Rs. Compensation for the loss of these inhibitory receptor subunit combinations is likely achieved by upregulation of $\alpha4\beta\gamma2$ and $\alpha5\beta\gamma2$ GABA$_A$Rs at synaptic and extrasynaptic locations, respectively. Extrasynaptic insertion of $\alpha4\beta\gamma2$ likely involves protein kinase C (PKC) phosphorylation of α4 subunits (Abramian et al. 2010), while insertion and clustering of $\alpha5\beta\gamma2$ is likely facilitated by the actin-binding protein radixin (Loebrich et al. 2006). The specific role of γ2 subunits in the membrane insertion, clustering, and localization to synaptic or extrasynaptic sites of CIE-induced $\alpha4\beta\gamma2$ and $\alpha5\beta\gamma2$ GABA$_A$Rs remains to be determined.

Previous studies demonstrated that extrasynaptic $\alpha5\beta\gamma2$ GABA$_A$Rs in the hippocampus are DZ sensitive; this sensitivity is eliminated by the introduction of δ or α4 subunits and reduced by substitution of γ2 with γ1 or γ3 subunits (reviewed in Möhler et al. 2000). The loss of DZ sensitivity of I_{tonic} in MSNs from CIE rats is consistent with the observed increases in α4, α5, and γ2 subunit levels in the NAcc of CIE rats and their likely assembly into $\alpha4\beta\gamma2$ or $\alpha5\beta\gamma2$ GABA$_A$Rs. It remains to be determined whether the protein levels of γ1 or γ3 subunits are increased in NAcc of CIE rats. However, increases in γ1 subunit mRNA have previously been reported in the cortex of chronic EtOH-treated rats (Devaud et al. 1995), as well as in the hippocampus of CIE rats (Cagetti et al. 2003). Interestingly, recent studies have demonstrated that replacing α1 with α2 and γ1 with γ2 at engineered GABAergic synapses results in slower mIPSC kinetics and produces a more diffuse clustering of GABA$_A$Rs containing these subunits (Dixon et al. 2014). Analogous subunit "switches" at MSN synapses after CIE treatment might contribute to the observed increases in rise time of mIPSCs, as an alternative to the proposed decrements in FS interneuron-MSN GABA release sites.

The lack of overall changes in the magnitude of I_{tonic} was surprising, compared with the large decreases observed in the hippocampus (Liang et al. 2007), but also consistent with the compensatory increases in α5 subunit content in the NAcc of CIE rats. The present study's demonstration of preferential EtOH sensitivity of I_{tonic} in MSN neurons from CIV rats is also consistent with the demonstration that selective reduction of the GABA$_A$R α4-subunit expression in the NAcc of rats, with virus-mediated RNAi techniques, reduces EtOH self-administration and preference and decreases the reinforcing effects of EtOH (Rewal et al. 2009, 2012). Selective reduction of the GABA$_A$R δ-subunit expression in NAcc also decreases EtOH intake (Nie et al. 2011). It is noteworthy that the decreases in low-to-moderate voluntary EtOH intake were selective for RNAi injections in the medial shell of the NAcc and not in the core (Nie et al. 2011; Rewal et al. 2009, 2012). In contrast, the NAcc core has been implicated in the reinstatement of conditioned alcohol seeking (Chaudhri et al. 2008) and in the aversion- and punishment-resistant aspects of alcohol dependence (Seif et al. 2013). The core of the NAcc was also implicated in locomotor sensitization to EtOH, which resulted in decreased NMDA receptor-dependent synaptic plasticity selectively in the core but not the shell, and increased EtOH consumption in mice (Abrahao et al. 2013). Further studies would be needed to determine the relative contributions of NAcc shell and core regions to the large increases in EtOH consumption observed after CIE treatment and withdrawal (Rimondini et al. 2002, 2003; Valdez et al. 2002).

In MSNs at their resting ("down") state, similar to hippocampal interneurons (Song et al. 2011), the GABA$_A$R current reversal potential is depolarizing, making baseline I_{tonic} excitatory. This was elegantly demonstrated in loose cell-attached recordings from striatal MSNs during activation of cortical glutamatergic inputs (Ade et al. 2008). In these recordings, excitatory synaptic activation of single action potentials in MSNs was reduced during application of L655,703, an α5 subunit GABA$_A$R-preferring modulatory inverse agonist ligand that preferentially antagonizes I_{tonic} in MSNs (Ade et al. 2008). Increasing I_{tonic} conductance in hippocampal interneurons was shown to enhance shunting-mediated inhibition, eventually overpowering excitation (Song et al. 2011). Analogously, acute EtOH administration should decrease excitability of MSNs in CIV rats via enhancement of extrasynaptic GABA$_A$R-mediated shunting inhibition. In contrast, the observed "switch" of EtOH sensitivity from I_{tonic} to synaptic currents in CIE rats suggests that only the shunting inhibition of phasic synaptic currents would be responsive to potentiation by acute EtOH in these alcohol-dependent rats.

Analysis of time-dependent alterations in the surface levels of select GABA$_A$R subunits in the NAcc after single doses of EtOH revealed increased internalization of α4 and δ subunits at 1 h after EtOH administration, without changes in α1 or γ2 subunits. These data provided further support for the internalization of extrasynaptic EtOH-sensitive $\alpha4\beta3\delta$ GABA$_A$Rs as an early event in the cycles of intoxication and withdrawal that eventually result in the persistent GABA$_A$R alterations of CIE rats (Liang et al. 2007; Shen et al. 2011). Recent studies in the hippocampus revealed that this internalization is detectable within 5 min of EtOH (3 g/kg ip) administration and involves increased association of δ subunit with clathrin adaptor proteins AP2-μ2 (Gonzalez et al. 2012). Increased phosphorylation of the β3 subunit was also observed but was not directly associated with the AP2 machinery. Since phosphorylation of the α4 subunit dictates its insertion into the membrane, rather than its endocytosis (Abramian et al. 2010; Werner et al. 2011), the precise mechanism of EtOH-induced $\alpha4\beta3\delta$ GABA$_A$R internalization remains to be elucidated.

In contrast with α4 and δ subunits, decreases in surface α1 subunits were not observed at 1 h after EtOH, but maximal decreases were seen at 2 days after EtOH, returning to control levels by 7 days after EtOH (Fig. 7). Similar delayed decreases were previously observed in the CA1 and dentate gyrus regions

Downloaded from on July 7, 2014

of the hippocampus after a single EtOH dose (Liang et al. 2007), and numerous investigators have reported long-lasting decreases in α1 subunit expression after chronic EtOH treatment in different brain regions (Cagetti et al. 2003; Devaud et al. 1995; Diaz et al. 2011; Mhatre and Ticku 1992; Morrow et al. 1990). Initial EtOH-induced decreases in surface α1-containing $GABA_ARs$ appear to involve selective increases in PKCγ activity, which in turn increases internalization of α1 $GABA_ARs$ (Kumar et al. 2010), while activation of PKA has opposing actions (Carlson et al. 2013). The mechanisms by which chronic EtOH exposure results in transcriptionally mediated decreases in α1 subunit content have yet to be determined. However, brain-derived neurotrophic factor (BDNF) and its downstream second messenger pathways have been implicated in status epilepticus-induced decreases in α1 (and increased α4) subunit gene expression (Brooks-Kayal and Russek 2012). Interestingly, chronic EtOH administration is associated with region-specific changes in BDNF expression (Davis 2008), and BDNF-mediated second messenger pathways in the dorsolateral striatum have been implicated in control of voluntary EtOH intake (Logrip et al. 2009).

At 2 days after single-dose EtOH, surface α4 and α5 subunit levels in the NAcc were significantly increased (Fig. 7) along with increases in surface γ2 levels (Fig. 8). Similar changes in α4 and γ2, but not α5, subunit levels were previously reported for the CA1 and dentate gyrus regions of the hippocampus in rats after single-dose EtOH (Liang et al. 2007). Therefore, the increases in α5 subunit levels appear to be specific to the NAcc. The mechanism of the transcriptionally driven increases in α4 was demonstrated to involve EtOH-induced activation of the heat shock immediate-early gene pathway elements to enhance the expression of Gabra4 and several other alcohol-responsive genes (Pignataro et al. 2007). Furthermore, selective PKCγ activation was shown to be required for EtOH-induced increases in membrane surface expression of α4 subunits in cultured cerebral cortical neurons (Werner et al. 2011). Presently it is unknown whether similar transcriptional and posttranscriptional mechanisms underlie the EtOH-induced increases in α5 and γ2 subunit levels in the NAcc.

At 2 days after single-dose EtOH the alterations in $GABA_AR$ surface subunit levels were remarkably similar to those observed in CIE rats, yet by 1–2 wk after the single EtOH dose surface levels of all examined subunits returned to control levels, whereas the increases were persistent in the NAcc of CIE rats (compare Figs. 6, 7, and 8). Numerous studies have shown that CIE treatment is particularly effective at producing long-lasting alterations in physiology and behavior; however, the mechanisms behind the persistence of CIE-induced alterations are only now beginning to be examined. There is evidence that epigenetic mechanisms may participate in EtOH-induced $GABA_AR$ plasticity (Pandey et al. 2008; Sakharkar et al. 2012). It would be of interest to examine whether similar epigenetic alterations may be present after CIE treatment in rats or in the brains of alcoholics.

Our present data point to a decrement in the presynaptic release and postsynaptic $GABA_AR$ receptor function in the NAcc of CIE rats. Previously, we demonstrated enhancement of α-amino-3-hydroxy-5-methyl-4-isoxazolepropionic acid receptor (AMPAR)-mediated glutamatergic neurotransmission in MSNs of CIE rats (Marty and Spigelman 2012). This potentiation of glutamatergic inputs should enhance the integration of dendritic excitability and increase the probability of action potential initiation at the soma, in effect increasing the likelihood of an "up" state, when NAcc neurons execute their behaviorally relevant functions (O'Donnell et al. 1999). The observed decrements in GABAergic neurotransmission should further contribute to the increased probability of an "up" state and also alter spike timing in favor of increased frequency of discharge, particularly given the faster spike repolarization and larger afterhyperpolarization also observed in the MSNs of CIE rats (Marty and Spigelman 2012). Action potential discharge during the "up" state constitutes the pertinent physiological coding event required for the induction of spike time-dependent plasticity (STDP), an activity-dependent long-term synaptic plasticity, that can bidirectionally modulate the strength of glutamatergic and GABAergic synaptic inputs in MSNs and interneurons (reviewed in Fino and Venance 2011). Moreover, GABAergic inhibition was recently demonstrated to govern the polarity of STDP, because blockade of $GABA_ARs$ was able to completely reverse the temporal order of plasticity at corticostriatal synapses in rats and mice, thus establishing a central role for GABAergic circuits in shaping STDP (Paille et al. 2013). The combined effect of the various alterations in MSNs of CIE rats is expected to greatly increase information transfer from areas such as the prelimbic cortex, hippocampus, and amygdala to the MSN GABAergic projections areas such as the ventral pallidum and the VTA. It is noteworthy that analogous decrements in GABAergic neurotransmission (Otaka et al. 2013), potentiated glutamatergic neurotransmission (Conrad et al. 2008), and enhanced action potential afterhyperpolarization (Mu et al. 2010) were observed after cocaine withdrawal, suggesting shared neurobiological mechanisms of dependence between alcohol and other drugs of abuse.

In summary, we demonstrated persistent decrements in GABAergic neurotransmission in NAcc core MSNs of rats during withdrawal from CIE treatment, a model of alcohol dependence. These include decreased synaptic release of GABA and alterations in $GABA_AR$ subunit composition, function, and pharmacological sensitivity to ligands, including EtOH. Together with the previously observed enhancement in glutamatergic neurotransmission (Marty and Spigelman 2012) and the modulatory influences of dopamine (see companion article, Liang et al. 2014) these alterations should result in greater signal throughput from MSNs in the NAcc core to their projection areas. Experiments using a combination of optogenetic and operant behavioral techniques could reveal the extent to which these CIE-induced alterations contribute to the compulsive and excessive EtOH intake in alcohol dependence.

ACKNOWLEDGMENTS

We thank Prof. Werner Sieghart (Medical University of Vienna, Vienna, Austria) for the generous supply of $GABA_AR$ subunit antibodies. We also thank Drs. Felix Schweitzer and Thomas Otis (Department of Neurobiology, UCLA) for help with data analysis and interpretation.

GRANTS

This work was supported by National Institute on Alcohol Abuse and Alcoholism Grants AA-016100 (I. Spigelman), AA-07680 (R. W. Olsen), AA-017991 (J. Liang), and AA-021037 (E. M. Meyer).

DISCLOSURES

No conflicts of interest, financial or otherwise, are declared by the author(s).

Downloaded from on July 7, 2014

AUTHOR CONTRIBUTIONS

Author contributions: J.L., R.W.O., and I.S. conception and design of research; J.L., A.K.L., A.S., E.M.M., V.N.M., S.O.A., and I.S. performed experiments; J.L., A.K.L., A.S., E.M.M., V.N.M., S.O.A., X.M.S., and I.S. analyzed data; J.L., A.K.L., A.S., E.M.M., V.N.M., S.O.A., X.M.S., R.W.O., and I.S. interpreted results of experiments; J.L., A.K.L., E.M.M., V.N.M., S.O.A., X.M.S., and I.S. prepared figures; J.L., A.K.L., V.N.M., X.M.S., R.W.O., and I.S. edited and revised manuscript; J.L., A.K.L., A.S., E.M.M., V.N.M., S.O.A., X.M.S., R.W.O., and I.S. approved final version of manuscript; I.S. drafted manuscript.

REFERENCES

Abrahao KP, Ariwodola OJ, Butler TR, Rau AR, Skelly MJ, Carter E, Alexander NP, McCool BA, Souza-Formigoni ML, Weiner JL. Locomotor sensitization to ethanol impairs NMDA receptor-dependent synaptic plasticity in the nucleus accumbens and increases ethanol self-administration. *J Neurosci* 33: 4834–4842, 2013.

Abramian AM, Comenencia-Ortiz E, Vithlani M, Tretter EV, Sieghart W, Davies PA, Moss SJ. Protein kinase C phosphorylation regulates membrane insertion of $GABA_A$ receptor subtypes that mediate tonic inhibition. *J Biol Chem* 285: 41795–41805, 2010.

Ade KK, Janssen MJ, Ortinski PI, Vicini S. Differential tonic GABA conductances in striatal medium spiny neurons. *J Neurosci* 28: 1185–1197, 2008.

Beckstead RM, Domesick VB, Nauta WJ. Efferent connections of the substantia nigra and ventral tegmental area in the rat. *Brain Res* 175: 191–217, 1979.

Bennett BD, Bolam JP. Synaptic input and output of parvalbumin-immunoreactive neurons in the neostriatum of the rat. *Neuroscience* 62: 707–719, 1994.

Brog JS, Salyapongse A, Deutch AY, Zahm DS. The patterns of afferent innervation of the core and shell in the "accumbens" part of the rat ventral striatum: immunohistochemical detection of retrogradely transported fluorogold. *J Comp Neurol* 338: 255–278, 1993.

Brooks-Kayal AR, Russek SJ. Regulation of $GABA_A$ receptor gene expression and epilepsy. In: *Jasper's Basic Mechanisms of the Epilepsies*, edited by Noebels JL, Avoli M, Rogawski MA, Olsen RW, Delgado-Escueta AV. New York: Oxford Univ. Press, 2012, p. 574–580.

Brown MT, Tan KR, O'Connor EC, Nikonenko I, Muller D, Luscher C. Ventral tegmental area GABA projections pause accumbal cholinergic interneurons to enhance associative learning. *Nature* 492: 452–456, 2012.

Brown N, Kerby J, Bonnert TP, Whiting PJ, Wafford KA. Pharmacological characterization of a novel cell line expressing human $\alpha4\beta3\delta$ $GABA_A$ receptors. *Br J Pharmacol* 136: 965–974, 2002.

Cagetti E, Liang J, Spigelman I, Olsen RW. Withdrawal from chronic intermittent ethanol treatment changes subunit composition, reduces synaptic function, and decreases behavioral responses to positive allosteric modulators of $GABA_A$ receptors. *Mol Pharmacol* 63: 53–64, 2003.

Carlson SL, Kumar S, Werner DF, Comerford CE, Morrow AL. Ethanol activation of protein kinase A regulates $GABA_A$ $\alpha1$ receptor function and trafficking in cultured cerebral cortical neurons. *J Pharmacol Exp Ther* 345: 317–325, 2013.

Chang HT, Kitai ST. Projection neurons of the nucleus accumbens: an intracellular labeling study. *Brain Res* 347: 112–116, 1985.

Chaudhri N, Sahuque LL, Cone JJ, Janak PH. Reinstated ethanol-seeking in rats is modulated by environmental context and requires the nucleus accumbens core. *Eur J Neurosci* 28: 2288–2298, 2008.

Conrad KL, Tseng KY, Uejima JL, Reimers JM, Heng LJ, Shaham Y, Marinelli M, Wolf ME. Formation of accumbens GluR2-lacking AMPA receptors mediates incubation of cocaine craving. *Nature* 454: 118–121, 2008.

Dahlström A, Fuxe K. Evidence for the existence of monoamine-containing neurons in the central nervous system. I. Demonstration of monoamines in the cell bodies of brain stem neurons. *Acta Physiol Scand* 62: SUPPL-55, 1964.

Davis MI. Ethanol-BDNF interactions: still more questions than answers. *Pharmacol Ther* 118: 36–57, 2008.

de Quidt ME, Emson PC. Distribution of neuropeptide Y-like immunoreactivity in the rat central nervous system. II. Immunohistochemical analysis. *Neuroscience* 18: 545–618, 1986.

Devaud LL, Smith FD, Grayson DR, Morrow AL. Chronic ethanol consumption differentially alters the expression of γ-aminobutyric $acid_A$ receptor subunit mRNAs in rat cerebral cortex: competitive, quantitative reverse transcriptase-polymerase chain reaction analysis. *Mol Pharmacol* 48: 861–868, 1995.

Diaz MR, Christian DT, Anderson NJ, McCool BA. Chronic ethanol and withdrawal differentially modulate lateral/basolateral amygdala paracapsular and local GABAergic synapses. *J Pharmacol Exp Ther* 337: 162–170, 2011.

Dixon C, Sah P, Lynch JW, Keramidas A. $GABA_A$ receptor α and γ subunits shape synaptic currents via different mechanisms. *J Biol Chem* 289: 5399–5411, 2014.

Fallon JH, Moore RY. Catecholamine innervation of the basal forebrain. IV. Topography of the dopamine projection to the basal forebrain and neostriatum. *J Comp Neurol* 180: 545–580, 1978.

Fino E, Venance L. Spike-timing dependent plasticity in striatal interneurons. *Neuropharmacology* 60: 780–788, 2011.

Gonzalez C, Moss SJ, Olsen RW. Ethanol promotes clathrin adaptor-mediated endocytosis via the intracellular domain of δ-containing $GABA_A$ receptors. *J Neurosci* 32: 17874–17881, 2012.

Grosshans DR, Clayton DA, Coultrap SJ, Browning MD. Analysis of glutamate receptor surface expression in acute hippocampal slices. *Sci STKE* 2002: L8, 2002.

Hussain Z, Johnson LR, Totterdell S. A light and electron microscopic study of NADPH-diaphorase-, calretinin- and parvalbumin-containing neurons in the rat nucleus accumbens. *J Chem Neuroanat* 10: 19–39, 1996.

Janssen MJ, Ade KK, Fu Z, Vicini S. Dopamine modulation of GABA tonic conductance in striatal output neurons. *J Neurosci* 29: 5116–5126, 2009.

Jia F, Pignataro L, Schofield CM, Yue M, Harrison NL, Goldstein PA. An extrasynaptic $GABA_A$ receptor mediates tonic inhibition in thalamic VB neurons. *J Neurophysiol* 94: 4491–4501, 2005.

Knoflach F, Benke D, Wang Y, Scheurer L, Luddens H, Hamilton BJ, Carter DB, Mohler H, Benson JA. Pharmacological modulation of the diazepam-insensitive recombinant γ-aminobutyric $acid_A$ receptors $\alpha4\beta2\gamma2$ and $\alpha6\beta2\gamma2$. *Mol Pharmacol* 50: 1253–1261, 1996.

Koob GF, Le Moal M. Neurobiological mechanisms for opponent motivational processes in addiction. *Philos Trans R Soc Lond B Biol Sci* 363: 3113–3123, 2008.

Koob GF, Sanna PP, Bloom FE. Neuroscience of addiction. *Neuron* 21: 467–476, 1998.

Koos T, Tepper JM, Wilson CJ. Comparison of IPSCs evoked by spiny and fast-spiking neurons in the neostriatum. *J Neurosci* 24: 7916–7922, 2004.

Korn H, Faber DS. Quantal analysis and synaptic efficacy in the CNS. *Trends Neurosci* 14: 439–445, 1991.

Kumar S, Suryanarayanan A, Boyd KN, Comerford CE, Lai MA, Ren Q, Morrow AL. Ethanol reduces $GABA_A$ $\alpha1$ subunit receptor surface expression by a protein kinase Cγ-dependent mechanism in cultured cerebral cortical neurons. *Mol Pharmacol* 77: 793–803, 2010.

Liang J, Marty VN, Mulpuri Y, Olsen RW, Spigelman I. Selective modulation of GABAergic tonic current by dopamine in the nucleus accumbens of alcohol-dependent rats. *J Neurophysiol* (April 9, 2014). doi:10.1152/jn.00564.2013.

Liang J, Suryanarayanan A, Abriam A, Snyder B, Olsen RW, Spigelman I. Mechanisms of reversible $GABA_A$ receptor plasticity after ethanol intoxication. *J Neurosci* 27: 12367–12377, 2007.

Liang J, Zhang N, Cagetti E, Houser CR, Olsen RW, Spigelman I. Chronic intermittent ethanol-induced switch of ethanol actions from extrasynaptic to synaptic hippocampal $GABA_A$ receptors. *J Neurosci* 26: 1749–1758, 2006.

Loebrich S, Bahring R, Katsuno T, Tsukita S, Kneussel M. Activated radixin is essential for $GABA_A$ receptor $\alpha5$ subunit anchoring at the actin cytoskeleton. *EMBO J* 25: 987–999, 2006.

Logrip ML, Janak PH, Ron D. Escalating ethanol intake is associated with altered corticostriatal BDNF expression. *J Neurochem* 109: 1459–1468, 2009.

Marty VN, Spigelman I. Long-lasting alterations in membrane properties, K^+ currents, and glutamatergic synaptic currents of nucleus accumbens medium spiny neurons in a rat model of alcohol dependence. *Front Neurosci* 6: 86, 2012.

McKeon A, Frye MA, Delanty N. The alcohol withdrawal syndrome. *J Neurol Neurosurg Psychiatry* 79: 854–862, 2008.

Mhatre MC, Ticku MK. Chronic ethanol administration alters gamma-aminobutyric $acid_A$ receptor gene expression. *Mol Pharmacol* 42: 415–422, 1992.

Mody I, Pearce RA. Diversity of inhibitory neurotransmission through $GABA_A$ receptors. *Trends Neurosci* 27: 569–575, 2004.

Möhler H, Benke D, Fritschy JM, Benson J. The benzodiazepine site of $GABA_A$ receptors. In: *GABA in the Nervous System: the View at Fifty Years*, edited by Martin DL, Olsen RW. Philadelphia, PA: Lippincott Williams & Wilkins, 2000, p. 97–112.

Downloaded from on July 7, 2014

Morrow AL, Montpied P, Lingford-Hughes A, Paul SM. Chronic ethanol and pentobarbital administration in the rat: effects on $GABA_A$ receptor function and expression in brain. *Alcohol* 7: 237–244, 1990.

Mossier B, Togel M, Fuchs K, Sieghart W. Immunoaffinity purification of γ-aminobutyric $acid_A$ ($GABA_A$) receptors containing γ_1-subunits. Evidence for the presence of a single type of γ-subunit in $GABA_A$ receptors. *J Biol Chem* 269: 25777–25782, 1994.

Mouton PR. *The Stereologer Handbook: Introduction to Unbiased Stereology*. Alexandria, VA: Systems Planning and Analysis, 2000.

Mu P, Moyer JT, Ishikawa M, Zhang Y, Panksepp J, Sorg BA, Schluter OM, Dong Y. Exposure to cocaine dynamically regulates the intrinsic membrane excitability of nucleus accumbens neurons. *J Neurosci* 30: 3689–3699, 2010.

Nauta WJ, Smith GP, Faull RL, Domesick VB. Efferent connections and nigral afferents of the nucleus accumbens septi in the rat. *Neuroscience* 3: 385–401, 1978.

Nie H, Rewal M, Gill TM, Ron D, Janak PH. Extrasynaptic δ-containing $GABA_A$ receptors in the nucleus accumbens dorsomedial shell contribute to alcohol intake. *Proc Natl Acad Sci USA* 108: 4459–4464, 2011.

Nie Z, Zorrilla EP, Madamba SG, Rice KC, Roberto M, Siggins GR. Presynaptic CRF1 receptors mediate the ethanol enhancement of GABAergic transmission in the mouse central amygdala. *ScientificWorldJournal* 9: 68–85, 2009.

O'Donnell P, Grace AA. Synaptic interactions among excitatory afferents to nucleus accumbens neurons: hippocampal gating of prefrontal cortical input. *J Neurosci* 15: 3622–3639, 1995.

O'Donnell P, Greene J, Pabello N, Lewis BL, Grace AA. Modulation of cell firing in the nucleus accumbens. *Ann NY Acad Sci* 877: 157–175, 1999.

Otaka M, Ishikawa M, Lee BR, Liu L, Neumann PA, Cui R, Huang YH, Schluter OM, Dong Y. Exposure to cocaine regulates inhibitory synaptic transmission in the nucleus accumbens. *J Neurosci* 33: 6753–6758, 2013.

Paille V, Fino E, Du K, Morera-Herreras T, Perez S, Kotaleski JH, Venance L. GABAergic circuits control spike-timing-dependent plasticity. *J Neurosci* 33: 9353–9363, 2013.

Pandey SC, Ugale R, Zhang H, Tang L, Prakash A. Brain chromatin remodeling: a novel mechanism of alcoholism. *J Neurosci* 28: 3729–3737, 2008.

Paxinos G, Watson C. *The Rat Brain in Stereotaxic Coordinates*. San Diego, CA: Academic, 1998.

Pignataro L, Miller AN, Ma L, Midha S, Protiva P, Herrera DG, Harrison NL. Alcohol regulates gene expression in neurons via activation of heat shock factor 1. *J Neurosci* 27: 12957–12966, 2007.

Pirker S, Schwarzer C, Wieselthaler A, Sieghart W, Sperk G. $GABA_A$ receptors: immunocytochemical distribution of 13 subunits in the adult rat brain. *Neuroscience* 101: 815–850, 2000.

Rewal M, Donahue R, Gill TM, Nie H, Ron D, Janak PH. Alpha4 subunit-containing $GABA_A$ receptors in the accumbens shell contribute to the reinforcing effects of alcohol. *Addict Biol* 17: 309–321, 2012.

Rewal M, Jurd R, Gill TM, He DY, Ron D, Janak PH. Alpha4-containing $GABA_A$ receptors in the nucleus accumbens mediate moderate intake of alcohol. *J Neurosci* 29: 543–549, 2009.

Rimondini R, Arlinde C, Sommer W, Heilig M. Long-lasting increase in voluntary ethanol consumption and transcriptional regulation in the rat brain after intermittent exposure to alcohol. *FASEB J* 16: 27–35, 2002.

Rimondini R, Sommer W, Heilig M. A temporal threshold for induction of persistent alcohol preference: behavioral evidence in a rat model of intermittent intoxication. *J Stud Alcohol* 64: 445–449, 2003.

Roberto M, Madamba SG, Moore SD, Tallent MK, Siggins GR. Ethanol increases GABAergic transmission at both pre- and postsynaptic sites in rat central amygdala neurons. *Proc Natl Acad Sci USA* 100: 2053–2058, 2003.

Room R, Babor T, Rehm J. Alcohol and public health. *Lancet* 365: 519–530, 2005.

Sakharkar AJ, Zhang H, Tang L, Shi G, Pandey SC. Histone deacetylases (HDAC)-induced histone modifications in the amygdala: a role in rapid tolerance to the anxiolytic effects of ethanol. *Alcohol Clin Exp Res* 36: 61–71, 2012.

Seif T, Chang SJ, Simms JA, Gibb SL, Dadgar J, Chen BT, Harvey BK, Ron D, Messing RO, Bonci A, Hopf FW. Cortical activation of accumbens hyperpolarization-active NMDARs mediates aversion-resistant alcohol intake. *Nat Neurosci* 16: 1094–1100, 2013.

Sesack SR, Grace AA. Cortico-basal ganglia reward network: microcircuitry. *Neuropsychopharmacology* 35: 27–47, 2010.

Shen Y, Lindemeyer AK, Spigelman I, Sieghart W, Olsen RW, Liang J. Plasticity of $GABA_A$ receptors following ethanol pre-exposure in cultured hippocampal neurons. *Mol Pharmacol* 79: 432–442, 2011.

Song I, Savtchenko L, Semyanov A. Tonic excitation or inhibition is set by $GABA_A$ conductance in hippocampal interneurons. *Nat Commun* 2: 376, 2011.

Spigelman I, Olsen RW, Liang J, Suryanarayanan A, Lindemeyer AK, Meyer EM, Shen Y, Bagnera R, Marty VN. Molecular and functional changes in receptors: GABA and chronic alcohol consumption. In: *Biological Research on Addiction: Comprehensive Addictive Behaviors and Disorders*. Oxford, UK: Elsevier/Academic, 2013, p. 219–230.

Sun C, Sieghart W, Kapur J. Distribution of α1, α4, γ2, and δ subunits of $GABA_A$ receptors in hippocampal granule cells. *Brain Res* 1029: 207–216, 2004.

Sundstrom-Poromaa I, Smith DH, Gong QH, Sabado TN, Li X, Light A, Wiedmann M, Williams K, Smith SS. Hormonally regulated $\alpha_4\beta_2\delta$ $GABA_A$ receptors are a target for alcohol. *Nat Neurosci* 5: 721–722, 2002.

Swanson LW. The projections of the ventral tegmental area and adjacent regions: a combined fluorescent retrograde tracer and immunofluorescence study in the rat. *Brain Res Bull* 9: 321–353, 1982.

Taverna S, van Dongen YC, Groenewegen HJ, Pennartz CM. Direct physiological evidence for synaptic connectivity between medium-sized spiny neurons in rat nucleus accumbens in situ. *J Neurophysiol* 91: 1111–1121, 2004.

Tepper JM, Wilson CJ, Koos T. Feedforward and feedback inhibition in neostriatal GABAergic spiny neurons. *Brain Res Rev* 58: 272–281, 2008.

Valdez GR, Roberts AJ, Chan K, Davis H, Brennan M, Zorrilla EP, Koob GF. Increased ethanol self-administration and anxiety-like behavior during acute ethanol withdrawal and protracted abstinence: regulation by corticotropin-releasing factor. *Alcohol Clin Exp Res* 26: 1494–1501, 2002.

Van Bockstaele EJ, Pickel VM. GABA-containing neurons in the ventral tegmental area project to the nucleus accumbens in rat brain. *Brain Res* 682: 215–221, 1995.

Vincent SR, Johansson O. Striatal neurons containing both somatostatin- and avian pancreatic polypeptide (APP)-like immunoreactivities and NADPH-diaphorase activity: a light and electron microscopic study. *J Comp Neurol* 217: 264–270, 1983.

Vincent SR, Johansson O, Hokfelt T, Skirboll L, Elde RP, Terenius L, Kimmel J, Goldstein M. NADPH-diaphorase: a selective histochemical marker for striatal neurons containing both somatostatin- and avian pancreatic polypeptide (APP)-like immunoreactivities. *J Comp Neurol* 217: 252–263, 1983.

Wallner M, Hanchar HJ, Olsen RW. Ethanol enhances $\alpha4\beta3\delta$ and $\alpha6\beta3\delta$ γ-aminobutyric acid type A receptors at low concentrations known to affect humans. *Proc Natl Acad Sci USA* 100: 15218–15223, 2003.

Wei W, Faria LC, Mody I. Low ethanol concentrations selectively augment the tonic inhibition mediated by δ subunit-containing $GABA_A$ receptors in hippocampal neurons. *J Neurosci* 24: 8379–8382, 2004.

Wei W, Zhang N, Peng Z, Houser CR, Mody I. Perisynaptic localization of δ subunit-containing $GABA_A$ receptors and their activation by GABA spillover in the mouse dentate gyrus. *J Neurosci* 23: 10650–10661, 2003.

Werner DF, Kumar S, Criswell HE, Suryanarayanan A, Alex FJ, Comerford CE, Morrow AL. PKCγ is required for ethanol-induced increases in $GABA_A$ receptor α4 subunit expression in cultured cerebral cortical neurons. *J Neurochem* 116: 554–563, 2011.

Wise RA. Dopamine, learning and motivation. *Nat Rev Neurosci* 5: 483–494, 2004.

Xia Y, Driscoll JR, Wilbrecht L, Margolis EB, Fields HL, Hjelmstad GO. Nucleus accumbens medium spiny neurons target non-dopaminergic neurons in the ventral tegmental area. *J Neurosci* 31: 7811–7816, 2011.

Zezula J, Fuchs K, Sieghart W. Separation of α1, α2 and α3 subunits of the $GABA_A$-benzodiazepine receptor complex by immunoaffinity chromatography. *Brain Res* 563: 325–328, 1991.

Zhou FM, Wilson CJ, Dani JA. Cholinergic interneuron characteristics and nicotinic properties in the striatum. *J Neurobiol* 53: 590–605, 2002.

Zimprich F, Zezula J, Sieghart W, Lassmann H. Immunohistochemical localization of the α1, α2 and α3 subunit of the $GABA_A$ receptor in the rat brain. *Neurosci Lett* 127: 125–128, 1991.

Downloaded from on July 7, 2014